Science of the Total Environment 927 (2024) 172220

Contents lists available at ScienceDirect

Science of the Total Environment

journal homepage: www.elsevier.com/locate/scitotenv

Uneven response of phytoplankton-bacteria coupling under Saharan dust pulse and ultraviolet radiation in the south-western Mediterranean Sea

Presentación Carrillo [a], Juan Manuel González-Olalla [a,*], Marco J. Cabrerizo [a,b], Manuel Villar-Argaiz [a,b], Juan Manuel Medina-Sánchez [a,b]

[a] Instituto Universitario de Investigación del Agua, Universidad de Granada, C/ Ramón y Cajal, nº4, 18071, Granada, Spain
[b] Departamento de Ecología, Universidad de Granada, Campus Fuentenueva s/n, 18071 Granada, Spain

HIGHLIGHTS

- Stressors interaction (UV, Saharan dust) modify phytoplankton-bacteria relationship.
- Bacterial carbon demand (BCD) exceeds excreted organic C by phytoplankton (EOC).
- Degree of uncoupling (BCD:EOC) negatively relates to ecosystem metabolic balance.
- Saharan dust × UVR promote the coupling (BCD:EOC < 1) in heterotrophic nearshore.
- Saharan dust × UVR promote the uncoupling (BCD:EOC > 1) in autotrophic open sea.

GRAPHICAL ABSTRACT

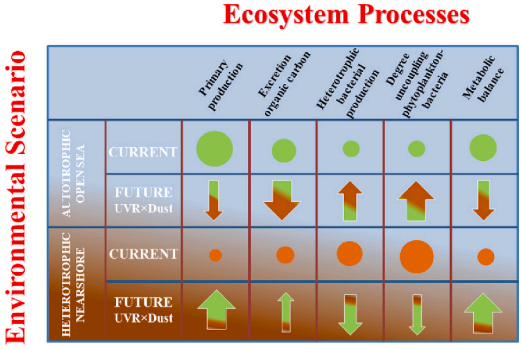

ARTICLE INFO

Editor: Olga Pantos

Keywords:
Heterotrophic bacterial carbon demand
Heterotrophic bacterial production
Primary production
Saharan dust pulse
Ultraviolet radiation

ABSTRACT

The microbial carbon (C) flux in the ocean is a key functional process governed by the excretion of organic carbon by phytoplankton (EOC) and heterotrophic bacterial carbon demand (BCD). Ultraviolet radiation (UVR) levels in upper mixed layers and increasing atmospheric dust deposition from arid regions may alter the degree of coupling in the phytoplankton-bacteria relationship (measured as BCD:EOC ratio) with consequences for the C-flux through these compartments in marine oligotrophic ecosystem. Firstly, we performed a field study across the south-western (SW) Mediterranean Sea to assess the degree of coupling (BCD:EOC) and how it may be related to metabolic balance (total primary production: community respiration; PP_T:CR). Secondly, we conducted a microcosm experiment in two contrasting areas (heterotrophic nearshore and autotrophic open sea) to test the impact of UVR and dust interaction on microbial C flux. In the field study, we found that BCD was not satisfied by EOC (i.e., BCD:EOC >1; uncoupled phytoplankton-bacteria relationship). BCD:EOC ratio was negatively related to PP_T:CR ratio across the SW Mediterranean Sea. A spatial pattern emerged, i.e. in autotrophic open sea stations uncoupling was less severe (BCD:EOC ranged 1–2), whereas heterotrophic nearshore stations uncoupling was more severe (BCD:EOC > 2). In the experimental study, in the seawater both enriched with dust and under UVR, BCD:EOC ratio decreased by stimulating autotrophic processes (particulate primary production (PP_P) and EOC) in the heterotrophic nearshore area, whereas BCD:EOC increased by stimulating heterotrophic processes

* Corresponding author.
E-mail addresses: pcl@ugr.es (P. Carrillo), jmolalla@ugr.es (J.M. González-Olalla), mjc@ugr.es (M. J. Cabrerizo), mvillar@ugr.es (M. Villar-Argaiz), jmmedina@ugr.es (J.M. Medina-Sánchez).

https://doi.org/10.1016/j.scitotenv.2024.172220
Received 27 November 2023; Received in revised form 21 March 2024; Accepted 2 April 2024
Available online 6 April 2024

[heterotrophic bacterial production (HBP), bacterial growth efficiency (BGE), bacterial respiration (BR)] in the autotrophic open sea. Our results show that this spatial pattern could be reversed under future UVR × Dust scenario. Overall, the impact of greater dust deposition and higher UVR levels will alter the phytoplankton-bacteria C-flux with consequences for the productivity of both communities, their standing stocks, and ultimately, the ecosystem's metabolic balance at the sea surface.

1. Introduction

Currently, climate change is causing an unprecedented increase in Earth's surface temperature of 0.9 °C from the 1960s (Calvin et al., 2023; IPCC, 2021). A crucial effect of global warming on aquatic ecosystems is a reduction in the depth of the upper mixed layer (UML) resulting from intensified thermal stratification in the water column (Sallée et al., 2021). The stratification reduces the flow of nutrients from deep waters into the UML, limiting nutrient availability for microbial growth (Gao et al., 2012; Kwiatkowski et al., 2020). Moreover, the shallowing of the UML traps microbial organisms in surface layers, increasing the photosynthetically active radiation (PAR) available for growth, but also exposing them to higher levels of damaging UVR (280–400 nm) (Williamson et al., 2019). Under these suboptimal solar radiation and nutrient-limiting conditions, the proportional excretion of organic carbon (%EOC) by phytoplankton may be enhanced (Carrillo et al., 2002, 2015a, 2015b; López-Sandoval et al., 2011; Marañón et al., 2004, 2005). However, knowledge concerning how EOC is processed by heterotrophic prokaryotes (hereafter bacteria) under stressful conditions in marine ecosystems remains scarce. This topic is timely because model predictions indicate that stratified nutrient-depleted regions will continue expanding with future warming (Behrenfeld et al., 2006; Moore et al., 2018; Sarmiento et al., 2004), affecting phytoplankton−bacteria commensalistic interaction, a key process based on the dependence of bacteria on EOC (Baines and Pace, 1991; Morán and Alonso-Sáez, 2011). Thus, the phytoplankton-bacteria relationship has been defined as coupled when EOC (carbon supply by phytoplankton) is sufficient to support the bacterial carbon demand (BCD) and uncoupled when BCD exceeds EOC. The prevalence of this interplay (coupling vs uncoupling) in the surface layers affects C-flux into the microbial loop (Thingstad et al., 1997), which balances the planktonic microbiome (Baetge et al., 2021; Cirri and Pohnert, 2019) and potentially, C sequestration in marine ecosystems through atmosphere-ocean transfer (Roshan and DeVries, 2017).

Climate-change research also predicts higher aeolian dust exportation from their origin sources (i.e., deserts and desertified areas), potentially increasing the supply of macronutrients —mainly nitrogen (N) and phosphorus (P) — and micronutrients —mainly iron (Fe)— to the sink ecosystems (Desboeufs et al., 2021; Hamilton et al., 2022; Jickells and Moore, 2015). Several studies evaluating the role of atmospheric deposition events have reported increases in particulate primary production (PP_P) (Gazeau et al., 2021a; Geisen et al., 2021; Lagaria et al., 2017; Marañón et al., 2010), heterotrophic bacterial production (HBP) (Guo et al., 2016), growth, and biomass production of phytoplankton and heterotrophic bacteria (González-Olalla et al., 2024; Maki et al., 2021; Zhou et al., 2021), as well as alterations in the structure of microbial planktonic communities (Borchardt et al., 2020), and C, N, P biogeochemical cycles (Djaoudi et al., 2018; Van Wambeke et al., 2020). However, a comprehensive understanding is still elusive concerning how the degree of coupling in the phytoplankton-bacteria relationship and the microbial processes implied in it are impacted by the joint action of UVR levels in surface water and increasing dust deposition over time (Cabrerizo et al., 2021; Chien et al., 2016). The interacting UVR and dust deposition effect in the UML may differ from their single and additive effects, altering the direction and magnitude of biological responses (non-additive effects: synergistic or antagonistic) (Galic et al., 2018; Gunderson et al., 2016).

The Mediterranean Sea is a low-nutrient, low-chlorophyll (LNLC) basin subjected to high-incident solar radiation (Durrieu de Madron et al., 2011) and highly exposed to Saharan dust deposition (Cerro et al., 2020). Previous studies indicate that the Mediterranean Sea is a P-limited system, so P availability can limit both PP and HBP (Céa et al., 2015; Marañón et al., 2021). However, available information on the dynamics of EOC and PP_P in surface Mediterranean waters (López-Sandoval et al., 2011; Santinelli et al., 2008) or BCD combined with microbial metabolism is scarce and limited to diverse narrow areas (Meador et al., 2010; Santinelli et al., 2013; van Wambeke et al., 2004). Even scarcer are studies combining information on C-flux links between these compartments, i.e., how PP_P or EOC are processed by bacterial metabolism (González-Benítez et al., 2019).

Based on oxygen budgets, it has been reported that the Mediterranean open-sea waters under stratified conditions function as net heterotrophic over large longitudinal gradients (Regaudie-De-Gioux et al., 2009). These authors discussed their findings in terms of a spatial and temporal decoupling between EOC by phytoplankton and BCD and/or by the input of DOC from the land and/or the atmosphere and/or surface circulation (Santinelli et al., 2012, 2021).

Currently, we lack direct empirical evidence that quantifies how Saharan dust inputs and UVR influence the coupling between EOC by phytoplankton and BCD, or how it may shift across temporal and spatial scales in environments with heterogeneous physical, chemical, and biological characteristics (Hewitt et al., 2007; Sandman et al., 2013; Serret et al., 2015). Previous results by our team reported that in heterotrophic nearshore areas Saharan dust inputs reduced (or inverted) the UVR damage on picoplanktonic PP (+antagonistic effect) but accentuated it in the autotrophic open areas (− synergistic effect) (Cabrerizo et al., 2016; González-Olalla et al., 2017). The consequences of these different sensitivities of autotrophic community on phytoplankton-bacteria commensalistic interaction are still unknown. We hypothesize that a future scenario of increased dust deposition under UVR will unevenly affect the phytoplankton-bacteria coupling: in the heterotrophic nearshore area of the Alborán Sea, PP_P and EOC will increase, favouring a coupled phytoplankton-bacteria relationship, whereas, in the autotrophic open sea, the accentuated UVR damage on PP (and EOC) will lead to insufficient EOC supply by phytoplankton to satisfy BCD, promoting an uncoupled phytoplankton-bacteria relationship).

From this background, we undertook the following steps: 1) a field study along transects covering the spatial heterogeneity of the physical-chemical characteristics of the SW Mediterranean Sea (Alborán Sea). The objective was to assess the degree of coupling in the phytoplankton-bacteria relationship and explore if BCD:EOC ratio relates to the metabolic balance of the ecosystem [total primary production ($PP_T = PP_P +$ EOC): community respiration (PP_T:CR)]; and 2) an experimental study, to quantify the magnitude and direction of the interaction Saharan dust pulse and UVR on microbial C-fluxes in two contrasting areas (heterotrophic nearshore and autotrophic open sea areas) over mid-term scales (5 days). Our final aim, through both approaches, was to study how a dust pulse under UVR may modify the degree of coupling in the phytoplankton-bacteria relationship and how this shift may relate to the expected future evolution of the metabolic balance in the SW Mediterranean Sea.

2. Material and methods

2.1. Field study

This study was carried out aboard the Spanish B. O. Francisco de Paula Navarro research vessel from 16 to 21 June 2014 (Fig. 1). The field study comprised a total of 14 stations over the SW Mediterranean Sea (hereafter Alborán Sea) to quantify the spatial heterogeneity of structure and metabolism of the microbial plankton communities. At each station, seawater samples from 5 and 15 m depth (inside the upper mixing layer) were collected using 10-L Niskin bottles and screened through 200-μm Nitex mesh to remove mesozooplankton (see below for a description of how the variables were measured).

2.2. Experimental study: setup of on-board incubations

Integrated samples from 0 to 15 m depth (300 L per area) in the autotrophic open sea (station 3; area inside the Western anticyclonic gyre, 35° 59′ N, 4° 19′ W; see Fig. 2a,b) and heterotrophic nearshore coastal areas (station 1; outside this gyre, 36° 37′ N, 4° 24′ W; see Fig. 2a, b) were collected to quantify the response of microbial plankton communities to the combined effect of a strong Saharan dust pulse and high UVR levels. To address this issue, we implemented a full factorial 2 × 2 design (in triplicate) with: (i) two radiation levels, PAR (Photosynthetically active radiation, > 400 nm, microcosms covered with Ultraphan UV 395 Opak Difegra film) and UVR + PAR, (>280 nm, microcosms covered with low-density polyethylene [LDPE] screen; Plásticos Andalucía, Spain); (ii) two dust levels, non-dust added (i.e. nutrient conditions at the sampling moment in each area) and Dust-added (i.e. enriched with 4.1 mg L^{-1} final concentration of Saharan dust). From

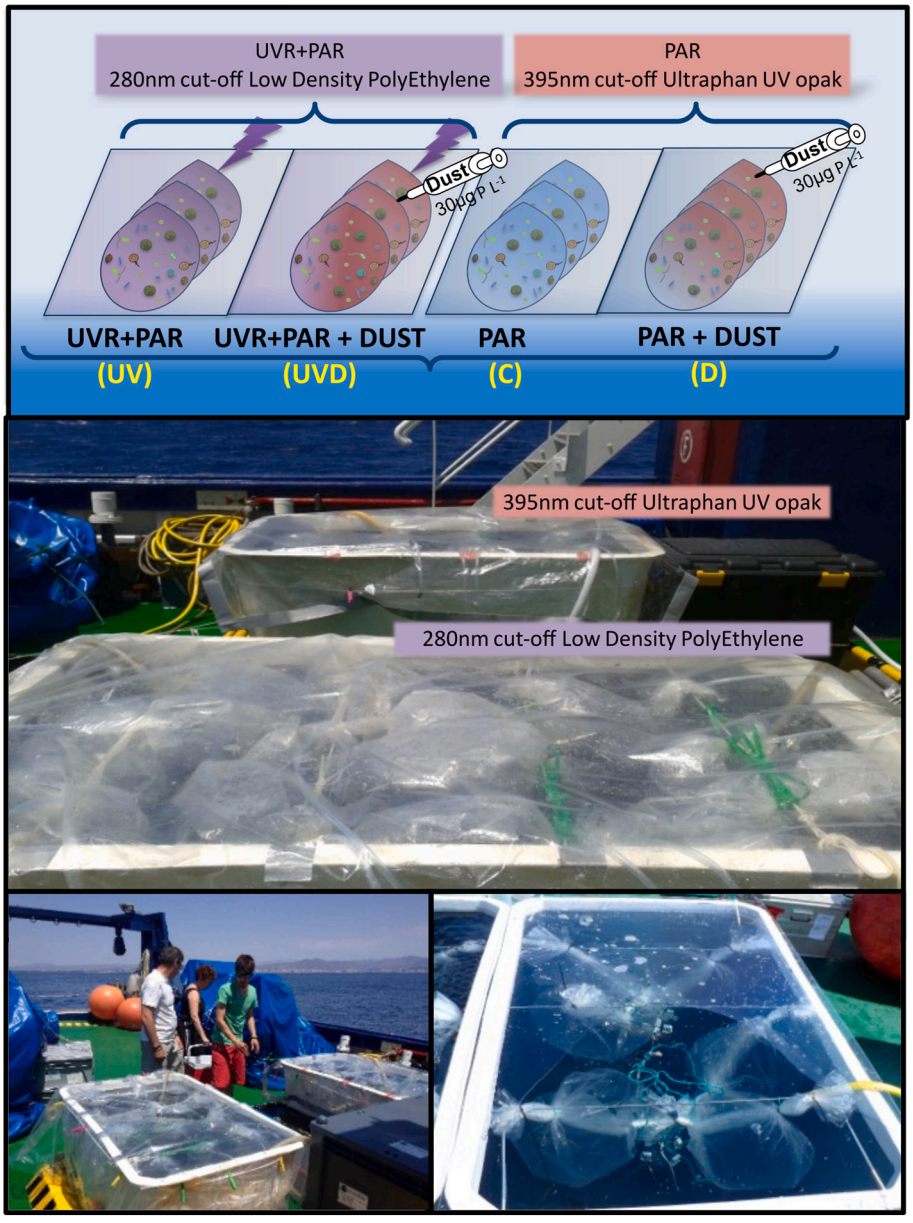

Fig. 1. Experimental design carried out aboard the Spanish Francisco de Paula Navarro research vessel from 16 to 21 June 2014. A total of 4 treatments were established to test the effect of UVR and dust (UV, UVD, C, and D treatments). Microcosms were covered with Ultraphan UV 395 Opak Difegra film in treatments incubated under PAR (Photosynthetically Active Radiation), and with Low-Density PolyEthylene (LDPE) screen in treatments incubated under PAR + Ultraviolet Radiation (UVR).

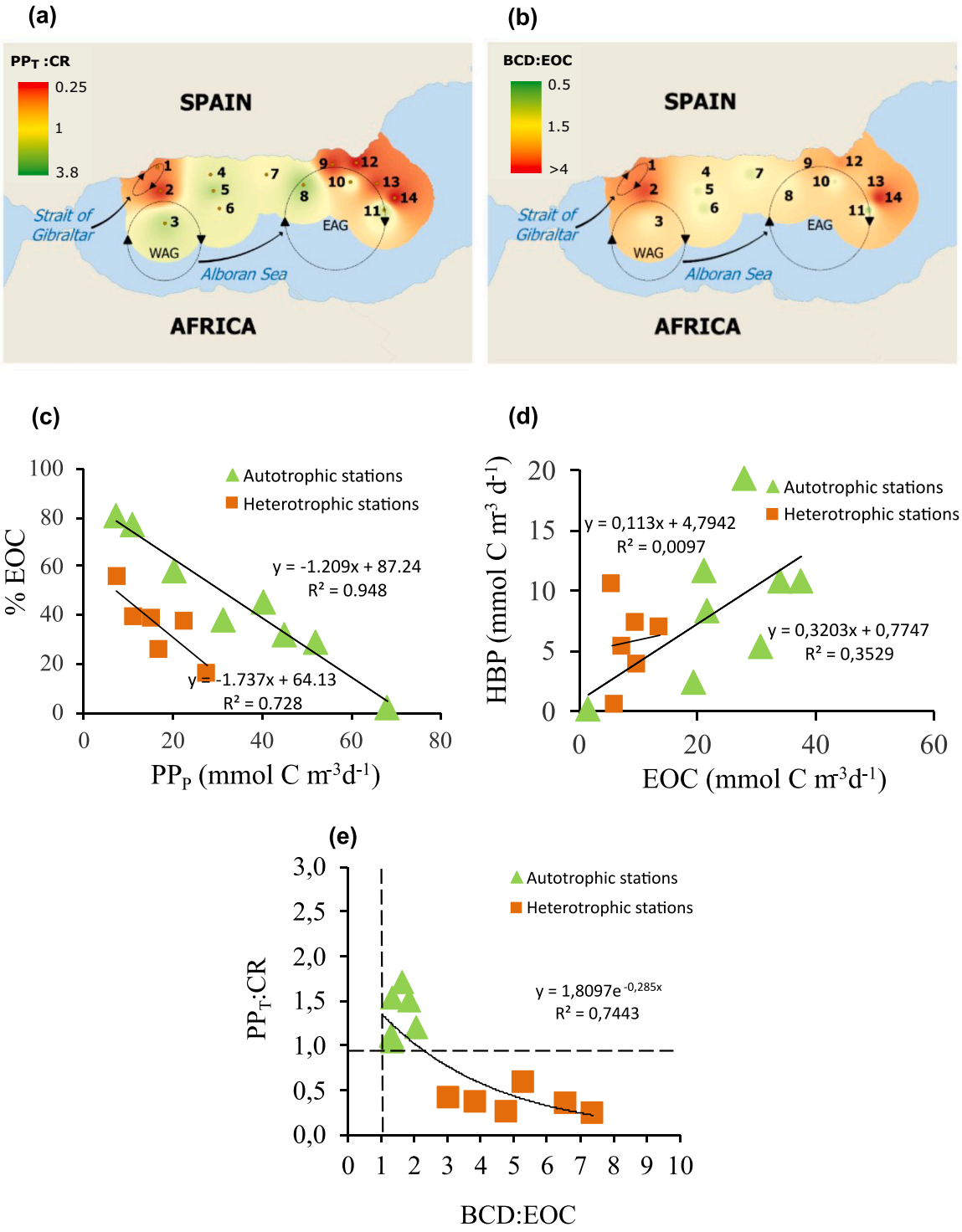

Fig. 2. Spatial pattern of a) metabolic balance (PP_T: CR ratio) and b) phytoplankton- bacteria commensalistic interaction (BCD: EOC ratio) along the Alboran Sea region. Numbers represent the location of sampling stations. The value of each variable, in each station, has an area of influence of 20 Km. The dotted grey lines represent the Western Anticyclonic Gyre (WAG) and Eastern Anticyclonic Gyre (EAG) and the coastal currents. Note that gyres are represented in relative magnitude and shape. Regressions between c) particulate primary production (PP_T) and excreted organic carbon as a percentage (%EOC), and d) EOC and heterotrophic bacterial production (HBP) in autotrophic open sea sites (green triangle) and Heterotrophic nearshore sites (orange square). Fitted solid line represents a significant ($p < 0.05$) linear regression model, and R^2 is the determination coefficient. e) Regression between phytoplankton-bacteria commensalistic interaction (BCD: EOC ratio) and metabolic balance (PP_T: CR ratio) in the SW Mediterranean Sea. Fitted solid line represents a significant ($p < 0.05$) exponential model, and R^2 is the determination coefficient.

above, four treatments (C, UV, D, and UVD) were named (Fig. 1). The Saharan dust was collected in the Tafilalet region of Morocco (31°06′00″ N, 3°59′24″ W). The dust addition (61.5 mg of dust per microcosm; 4.1 mg L^{-1}) mimics a realistic Saharan dust deposition to the Mediterranean region releasing 0.97 ± 0.17 μM of P (Lekunberri et al., 2010). The LDPE used transmits 90 % of photosynthetic active radiation, 75 % of UV-A, and 60 % of UV-B, whereas Ultraphan UV 395 Opak Difegra film transmits >90 % of PAR but screens out all UVR (< 390 nm). The procedure to obtain the Saharan dust with a mean range of particle size between 1 and 10 μm (i.e., the major fraction entering surface waters) has previously been described in detail (Cabrerizo et al., 2016).

The integrated seawater samples from each area [autotrophic open sea (station 3) and heterotrophic nearshore area (station 1)] were placed in two different opaque containers (150 L), one with ambient nutrient concentrations and the other enriched with Saharan dust, as described above. After dust addition, the seawater from each area and dust condition was distributed into 12 LDPE microcosms of 15-L capacity (2 × 2 treatments × 3 replicates, per each area). Once the microcosms were filled, they were suspended in two large black-painted tanks (c. 800 L each) placed on the ship deck. Half of the microcosms (6 from each area) were randomly placed in one of the tanks covered with LDPE film (UVR treatment), and the other half in another tank covered with Ultraphan UV 395 Opak Difegra film (C treatment). The microcosms were manually shaken (inside tanks) to avoid organisms settling and allowing them to receive homogeneous irradiance, and the temperature in both tanks was controlled by continuously pumping surface seawater. Incubations lasted 5 days, and sub-samples from each microcosm were taken every day at noon using a manual vacuum syringe connected to an acid-washed silicone tube inserted in each microcosm.

2.3. Physical-chemical-biological characterization of Alboran Sea

Incident solar radiation was continuously monitored through a BIC radiometer (*deck unit*, Biospherical Instruments Inc., CA, USA) with three channels in the UVR region of the spectra (305, 320, and 380 nm) and one broad-band channel for PAR (400–700 nm) installed on the ship deck. At each station, vertical profiles of solar radiation in the water column (down to 25 m) were also measured at noon using a BIC radiometer (*underwater unit*) with temperature and depth sensors in addition to the aforementioned channels. Diffuse attenuation coefficients for downward irradiance (k_d) were calculated from the slope of the linear regression of the natural logarithm of downwelling irradiance vs. depth for the different radiation bands. Likewise, vertical profiles of pH, salinity, and conductivity (0–25 m) were recorded using a sea logger CTD SBE 25 (Sea-Bird Electronics, Inc., WA, USA).

2.4. Nutrient analyses

At each station and for each microcosm, seawater samples were collected in 300 mL polyethylene terephthalate (PET) bottles and frozen (−20 °C) until total phosphorus (TP) and total nitrogen (TN) analyses. The samples for total dissolved nitrogen (TDN) and total dissolved phosphorus (TDP) were filtered through GF/F Whatman filters (Whatman Inc. UK 25 mm diameter) before freezing them. All nutrient (total and dissolved N and P) samples were subjected to persulphate oxidation and analysed following the spectrophotometric method (Koroleff, 1977). The detection limits for N and P were 0.08 μM and 0.03 μM, respectively, while the reproducibility ranged from 2.3 % to 5.4 %.

2.5. Chlorophyll a concentration (Chl a)

Samples from each station (3 L) and microcosm (3 L on June 17th, 1 L the following days; samples taken every day at noon) were filtered onto Whatman GF/F filters (25 mm in diameter), and frozen at −20 °C until analysed. At the laboratory, the photosynthetic pigments were extracted in absolute methanol in darkness at 4 °C for 24 h (Jeffrey and Humphrey, 1975) and measured using a fluorometer (Perkin Elmer, model LS 55). A Chl *a* standard (Chl *a* from spinach, Sigma-Aldrich) was used to transform the fluorescence data into Chl *a* concentration.

2.6. Heterotrophic bacterial abundance (HBA)

HBA was determined by flow cytometry (FACSCanto II, Becton Dickinson Biosciences, Oxford, UK), after fixing 1.5 mL of water samples from each station and microcosm with 75 μL of particle-free 20 % (*w/v*) glutaraldehyde (1 % final concentration) and immediately frozen in liquid nitrogen until analysis. Samples were thawed and stained with Syber Green I DNA (Sigma-Aldrich) at a final dilution of 1:5000 from the initial stock, and control samples without Syber Green I DNA were included for each treatment as fluorescent blanks. Yellow-green beads solution (Fluoresbrite Microparticles 1 μm, Polysciences, USA) at standard concentration (1 × 10^5 particles mL^{-1}) were added to determine bacterial abundance (Cabrerizo et al., 2016).

2.7. Particulate primary production and excreted organic carbon by phytoplankton

PP_P was measured by assessing the ^{14}C incorporation by phytoplankton cells (Steemann-Nielsen, 1952). Briefly, sets of 4 (3 clear replicates +1 dark control per station x depth or per experimental treatment x area) FEP narrow-mouth Teflon bottles (40 mL, Nalgene®, USA) filled with the corresponding water sample were inoculated with 5 μCi of $NaH_{14}CO^3$ (specific activity: 4.2 mCi $mmol^{-1}$, DHI Water and Environment, Germany), and incubated during 4 h centered at noon in tanks under the same conditions as with the microcosms. PP_P was determined by filtering 30 mL through GF/F filters (Whatman Inc. UK), under low vacuum (< 100 mmHg) to minimize cell breakage. EOC was measured on 4-mL aliquots from the filtrates (< 0.7 μm). The filters as well as the filtrates were placed in 20-mL scintillation vials and acidified with 100 μL of 1 N HCl for 24 h (no bubbling) to remove inorganic radiocarbon before the addition of a liquid-scintillation cocktail (Ecoscint A, National Diagnostics®, USA) to the vials. The amount of excreted organic carbon (EOC) in each fraction was determined by counting disintegrations per min, using an auto-calibrated scintillation counter (Beckman LS 6000 TA). In all the calculations, dark values were subtracted from the corresponding clear ones. The total CO_2 in the seawater was calculated from alkalinity and pH measurements (APHA, 2017). The percentage EOC was calculated as % EOC = 100 × (EOC:PP_T) with the total primary production (PP_T) obtained as the sum of PP_P and EOC. All daily rates were calculated by multiplying hourly rates by 12 light hours per day.

2.8. Heterotrophic bacterial production (HBP)

HBP was measured following the ^3H-thymidine method (Smith and Azam, 1992). Briefly, sets of 5 (3 replicates +2 blanks per station x depth or per experimental treatment x area) sterile microcentrifuge tubes filled with 1.5 mL of the corresponding water sample were inoculated with ^3H-thymidine (S.A. = 52 Ci $mmol^{-1}$, Perkin Elmer, USA) to a final saturating concentration of 15.2 nM. The tubes were then incubated at the in situ temperature of each station or treatment in the dark for 1 h. Although the consequence of incubations in the microcentrifuge tubes is that the samples were not under the UV-effect during the incubation time with ^3H-Thymidine, it did provide a snapshot of the status of bacteria growth due to the accumulative exposure to light conditions (e.g., UVR + PAR or only PAR). After incubation, the incorporation of ^3H-thymidine was stopped by adding trichloroacetic acid (TCA) at 5 % final concentration. Likewise, blanks were TCA-killed before the radiotracer was added. After the cold TCA extraction (20 min at <1 °C), the precipitate was collected by centrifugation at 16000*g* for 10 min, rinsed twice with 5 % TCA, and measured in an auto-calibrated scintillation counter (Beckman LS 6000 TA). The conversion factor 1.5 × 10^{18} cell mol^{-1} was used to estimate the number of HB produced per mol of

incorporated ^{3}H-thymidine (Bell, 1983). The factor 20 fg C cell^{-1} was applied to convert HBP into C terms (Lee and Fuhrman, 1987). Daily rates were calculated by multiplying hourly rates by 24 h per day.

2.9. Respiration rates

Microbial plankton community respiration (CR; <200 μm fraction) and bacterial respiration (BR; <0.7 μm fraction, GF/F Whatman Inc., UK) were determined on 40-mL UV-transparent Teflon FEP narrow-mouth bottles (Nalgene, USA) equipped with sensor spots (SP-PSt3-NAU-D5-YOP), filled with the corresponding unfiltered (CR) or filtered (BR) water sample, sealed to avoid gas exchange, and incubated in darkness to measure the oxygen concentration during 12 h using an oxygen transmitter (Fibox 3, Presens GmbH, Germany) equipped with Oxyview 6.02 software to register data. The system was calibrated by a two-point calibration, together with data of atmospheric pressure and temperature before each experiment. The limit of O_2 detection for our method was 0.47 μmol O_2 L^{-1}. Measurements were made at the initial time (t_0) and then every 3 h for 12 h. Oxygen data were then adjusted to a linear model via least-squares regression. The slope of the regressions provided the oxygen consumption rates (μM O_2 h^{-1}) (Medina-Sánchez et al., 2017). Oxygen was converted into carbon units using a respiratory quotient of 1 (del Giorgio and Cole, 1998). Daily rates were calculated by multiplying hour rates 24 h per day.

From the respiration measurements, we calculated: (i) the BCD as the sum of HBP and BR; (ii) the bacterial growth efficiency (BGE), i.e. the proportion of C entering the HBP pool that is converted into the biomass, as the ratio between HBP and BCD; (iii) the metabolic balance of the ecosystem as the ratio between PP_T and CR; and (iv) the degree of coupling of phytoplankton-bacteria as the ratio between BCD and EOC (i.e. uncoupling: BCD:EOC >1; coupling: BCD:EOC <1).

2.10. Data calculation and statistical analyses

Maps of physical-chemical parameters and biological variables in the Alborán Sea were created using QGIS software, Quantum Geographic Information System (version 3.16.15-Hannover, 2020). The maps were drawn by means of interpolation for the parameters or variables considered at each station point using an inverse distance-weighted technique. We chose this interpolation technique because it weights the influence of stations on an unknown point as a function of their distance (the closer, the more influence).

To quantify the magnitude and direction of the single and interactive effect of the two factors (UVR and Dust), we calculated the effect size of UVR, Dust and their interaction on PP_P, EOC, HBP, BR, BGE, and BCD: EOC ratio at each day of the experiment as:

$$\text{Effect size of UVR}\ (\%) = 100 \times ((\text{UV} - \text{C})/\text{C})$$

$$\text{Effect size of Dust}\ (\%) = 100 \times ((\text{D–C})/\text{C})$$

$$\text{Interactive effect size of UVR} \times \text{Dust}\ (\%) = 100 \times ((\text{UVD–C})/\text{C})$$

A positive effect size indicates that the factor(s) had a stimulatory effect on the response variable; conversely, a negative effect size indicates an inhibitory effect.

For each response variable, the nature of the effect UVR × Dust was determined following the procedure described by Piggott et al. (2015) by comparing the values of the interactive treatment (UVD) with their expected additive value, calculated as the sum of the individual effects i.e., C + (UV — C) + (D — C) for each day during the incubation period. The nature of the interactive effect was defined following Piggott et al. (2015) (Fig. 2 therein). A positive synergistic interaction was defined as the case in which the value of the combined treatment (UVD) is higher than the expected additive value and greater than the absolute value of each individual treatment. A negative antagonistic interaction was defined as the case in which the value of the combined treatment (UVD) is greater than the expected additive value but less (or equal) than the absolute value of the highest individual treatment. By contrast, a positive antagonistic interaction was defined as the case in which the value of the combined treatment (UVD) is less than the expected additive value but higher (or equal) than the absolute value of the lowest individual treatment. Finally, the negative synergistic interaction was defined as the case in which the value of the combined treatment (UVD) was lower than the expected additive value and lower than the absolute value of all individual treatments. Finally, we calculated the strength of the UVR × Dust interaction as the quotient between UVD and C treatment at the end of incubation time.

For the field study, non-linear (exponential) regression analysis between the BCD:EOC ratio and PP_T: CR ratio was performed. Single regression analyses were made to assess the relationship between the % EOC and PP_P. The normal distribution of residues in all regressions was checked by the Kolmogorov-Smirnov test.

For the experimental study, and for each area separately (heterotrophic nearshore and autotrophic open sea), a two-way repeated-measures analysis of variance (two-way RM-ANOVA) was used to test the effect of UVR, Dust pulse, and their interaction over time on all response variables quantified (i.e., TDN, TDP, Chl *a*, BA, BR, HBP, BGE, PP_P, EOC, BCD:EOC ratio). The assumptions on sphericity (determined by Mauchly's test) and homoscedasticity (by Levene's test) were checked, and when significant interactive effects were found, differences among and within treatments were assessed by Fisher's least-significant differences (LSD) post hoc test.

In addition, a one-way repeated-measures analysis of variance (one-way RM-ANOVA) was carried out to test the influence of Dust over time on the effect size of UVR (and the influence of UVR over time on the effect size of Dust) on each variable (PP_P, EOC, BR, HBP, BGE, BCD:EOC) for each area. LSD post hoc test was used to determine differences among and within treatments over the experiment. The statistical models were validated by checking the assumptions of sphericity determined by Mauchly's test and homoscedasticity by Levene's tests, respectively.

All variables expressed in absolute value are reported as mean values ± standard deviation, whereas error propagation was used to represent the variance of the effect size of UVR, Dust, and their interaction on all response variables. All analyses were performed with the STATISTICA v.7.0 software (Statsoft, 2007).

3. Results

3.1. Field study

The temperature of surface seawater (up to 25 m depth) followed a marked gradient across the study area (18–24 °C), the eastern Alborán Sea being warmer (mean values ~23.56 ± 0.22 °C) than the western (mean values ~18 ± 0.6 °C) (Fig. A1a). All stations showed high transparency to UVR (kd_{305} = 0.32–0.44, kd_{320} = 0.23–0.77, kd_{380} = 0.1–0.93 m^{-1}) and PAR (kd_{PAR} = 0.01–0.14 m^{-1}). Specifically, the eastern area was more transparent to UVR than the western area (kd_{320} = 0.15 vs. kd_{320} = 0.35 m^{-1}; Fig. A1b). Nutrient concentrations were low (Table A1a; TDP, mean values <0.65 μM), particularly in the eastern area of Alborán Sea (mean value 0.40 μM). TDN showed values ranging between 92 and 216 μM across the study section (Table A1a).

With respect to biological variables, the Chl *a* concentration was notably low, with values below 1 mg m^{-3} in 72 % of the stations and in no case exceeded ~2.5 mg Chl *a* m^{-3} (Fig. A1d). The PP_P varied between 7 (±1) and 68 (±1) mmol C m^{-3} d^{-1}, showing a clear spatial pattern with the lowest values in the eastern Alborán Sea (Fig. A1e). The EOC varied between 1.7 (±1) and 37.5 (±1) mmol C m^{-3} d^{-1} and followed an opposite spatial pattern to PP_P through the study area, with lower values (< 5 mmol C m^{-3} d^{-1}) in the western Alborán Sea (Fig. A1f; Table A1a). A negative exponential %EOC-PP_P regression (%EOC = 55.97 e$^{-0.023}$ PP_P; R^2 = 0.49) was found for all stations together. When the stations

were divided according to values of the metabolic balance (PP_T:CR >1, net autotrophic metabolism; PP_T:CR <1, net heterotrophic metabolism) (Table A1a), the %EOC-PP_P regression turned to significantly linear, with comparatively higher values %EOC in autotrophic sites (Fig. 2c).

As EOC, the lowest values for the HBP and BA spatial distribution were found in the western Alborán Sea (Fig. A1g, h). The weak HBP vs. EOC relationship (Fig. 2d), and BCD:EOC ratio over 1 (1.3 and 7.4) are indicative of an uncoupled phytoplankton-bacteria relationship in the Alborán sea, however, the degree of this uncoupling ranged from weakly-uncoupled (BCD:EOC, range 1–2) to strongly uncoupled (BCD: EOC >2) areas (Fig. 2b; Table A1a). The spatial response pattern is consistent with that of the PP_T:CR ratios (Fig. 2a; Table A1a), indicating that in strongly-uncoupled stations (BCD:EOC >2), the PP_T: CR ratio exhibited values <1 (i.e. net heterotrophic area) whereas in weakly-uncoupled stations (BCD:EOC ≤ 2), the PP_T:CR values were > 1 (i.e., autotrophic area) (Fig. 2a,b, Table A1a). Thus, a significant negative exponential BCD:EOC vs. PP_T:CR regression was established (Fig. 2e): where uncoupling was weaker (BCD:EOC was closer to 1), the ecosystem was net autotrophic and could behave as a C-sink, whereas where uncoupling was stronger (BCD:EOC > 2), the ecosystem was net heterotrophic and could act as a C-source for the atmosphere (Fig. 2e).

3.2. Experimental study

3.2.1. Physical and chemical conditions in autotrophic open sea and heterotrophic nearshore areas

Mean daily irradiance range during the experiment was 2.03–2.82 μW m^{-2} for 305 nm, 15.60–19.30 μW cm^{-2} for 320, and 41.60–52.30 μW cm^{-2} for 380 nm, and 225.60–282.30 W m^{-2} for PAR (Fig. A2). The high TDN and low TDP in C and UV treatments indicate a strong P-

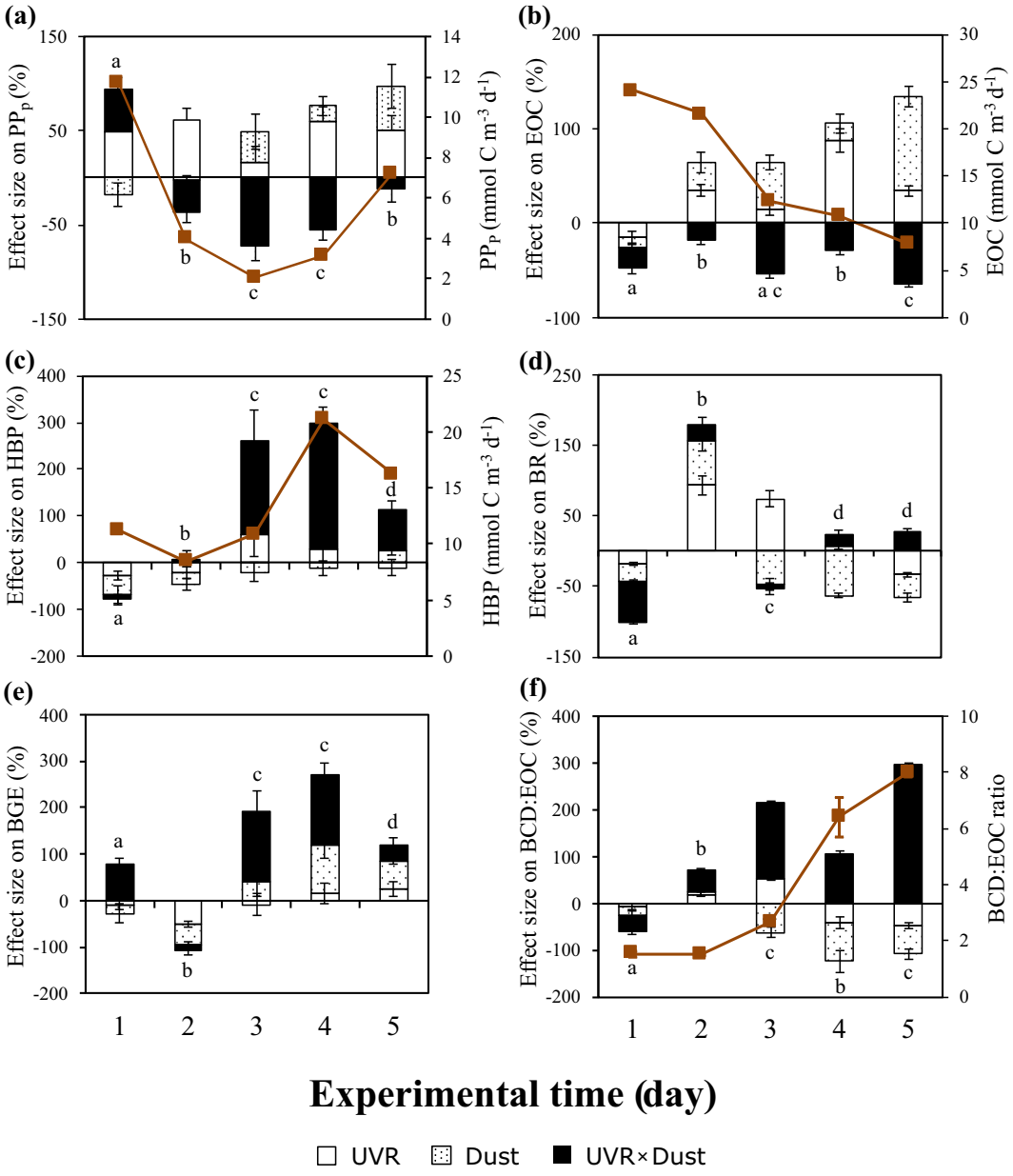

Fig. 3. The effect size of UVR, Dust, and UVR × Dust on metabolic variables from the autotrophic open-sea area. Figure includes (a) particulate primary production (PP_P), (b) excretion of organic carbon by phytoplankton (EOC), (c) heterotrophic bacterial production (HBP), (d) bacterial respiration (BR), (e) bacterial growth efficiency (BGE), and (f) bacterial carbon demand: excretion of organic carbon (BCD: EOC) ratio. Each segment in a stacked bar represents the mean values of three replicates, while the vertical lines indicate the standard deviation for each factor UVR, Dust, and UVR × Dust. The letters indicate differences among UVR × Dust treatment by LSD post hoc test over the experiment. The brown line links mean values of the corresponding variable under UVR × Dust treatment.

limitation in both experimental areas (Table A1b), and dust addition enhanced the P availability (Fig. A3).

3.2.2. Joint effects of dust and UVR on phytoplankton and heterotrophic bacterial metabolism in autotrophic open sea area

PP_P slightly increased in all treatments except under the UVD treatment, where a significant decrease (U-shaped) occurred over time (Fig. A4a, Table A2a). The effect size of UVR on PP_P had a consistent pattern of positive values over the experiment whereas the effect size of Dust on PP_P showed negative values at the beginning of the experiment but was positive toward the end of the experimental period (Fig. 3a). The effect size of UVR × Dust on PP_P followed a pattern inverse to that of the single effect size of Dust, from positive values at first day to negative values over the experiment (Fig. 3a).

EOC values showed opposite responses in the two Dust treatments. Thus, in UVD treatment, EOC decreased by 75 % over the experiment, whereas in D treatment EOC underwent a significant increase over time (post hoc, Fisher's LSD $p < 0.05$) (Fig. A4b, Table A2a). The single effect sizes of UVR and Dust on EOC changed from negative on the first day to strongly positive over the experiment. However, the effect size of UVR × Dust on EOC was consistently negative regardless of the temporal scale (Fig. 3b).

HBP decreased after the first day of the experiment in all treatments but significantly increased, particularly in UVD, at the end of the experiment (Fig. A4c, Table A2a). Hence, the effect size of UVR × Dust on HBP was positive after the second day of the experiment (Fig. 3c). BR and BGE showed no clear response pattern to the factors tested over the experiment (Fig. 3d,e), though BGE showed a higher mean value in UVD treatment (Fig. A4d,e). As for HBP, the effect size of UVR × Dust on BGE was positive (except at day 2, Fig. 3). Overall, UVR × Dust had a negative synergistic effect, inhibiting PP_P and EOC, whereas it had a stimulatory effect on bacterial variables (positive synergistic effect on HBP, and negative antagonistic effect on BR and BGE (Table 1a).

The BCD:EOC ratio showed values of >1 in almost all the treatments over the experiment. Nevertheless, it is noticeable the progressive increase of BCD: EOC values under UVD conditions from 1.5 in the first two days to 8.0 at the end of the experiment (Fig. A4f). This indicates that bacteria under two stressors experimented progressively higher limitation by C-released by phytoplankton. The effect size of UVR × Dust on BCD: EOC varied from negative values (both factors enhanced phytoplankton-bacteria C-flux, becoming less uncoupled) to significantly positive values (both factors diminished phytoplankton-bacteria C-flux, becoming more uncoupled) (Fig. 3f, Table A3a,b). The nature of the UVR × Dust interaction was a positive synergism (both factors augmented the BCD:EOC ratio, becoming more uncoupled) (Table 1a). At a structural level, Chl *a* concentration increased in all treatments up to day 4, with significant differences among days (Fig. A5a; UVR × Dust×Time $p < 0.05$, Table A2b) but BA significantly increased only under UVD condition over the experiment (Fig. A5c, Table A2b).

3.2.3. Joint effects of dust and UVR on algal and bacterial metabolism in the heterotrophic nearshore area

The PP_P significantly increased in all treatments (except for C), with values ranging between ~2 at the beginning (D treatment) and up to ~12 mmol C m^{-3} d^{-1} (UVD treatment) at the end of the experiment (Fig. A6a, Table A2a). The effect sizes of UVR, Dust, and UVR × Dust on PP_P were negative during the two first days but became strongly positive at the end of the experiment (Fig. 4a, Table A3b). As for PP_P, EOC significantly increased in all treatments, ranging from ~5 at the beginning and up to peak values of ~45 mmol C m^{-3} d^{-1} (UV treatment) at the end of the experiment (Fig. A6b, Table A2a). Single and interactive effect sizes of UVR and Dust on EOC followed a similar response pattern than that of PP_P (from negative to positive values over the experiment; Fig. 4b, Table A3b). Overall, HBP decreased in all treatments over the experiment (Fig. A6c). Nevertheless, HBP was significantly higher in D and UVD than in the treatments without Dust, showing the lowest values in the C treatment, although these differences among treatments disappeared at the end of the incubation period (UVR × Dust×Time $p < 0.05$, Table A2a). The effect sizes of UVR, Dust, and UVR × Dust on HBP were positive (except UVR × Dust on day 5; Fig. 4c). Although BR and BGE followed no clear response pattern to the factors (except BGE to UV; Fig. A6d,e), the effect size of UVR × Dust on these variables was positive in most of these cases (except BR on day 5; Fig. 4d,e). The nature of UVR × Dust interaction was positive antagonism for PP_P, EOC, HBP and BGE or positive synergistic on BR, i.e., a stimulatory effect on these response variables, whereas it was negative synergistic i.e., inhibitory effect, on BCD: EOC ratio (Table 1b). The BCD: EOC ratio significantly decreased under almost all experimental conditions over the experiment, and

Table 1
Types of interactive effects between ultraviolet radiation UVR and Dust, calculated from the magnitude and direction of the additive effect and interactive effect on algal and bacterial metabolic variables for the average-time of effect sizes over the incubation period. a) Autotrophic open-sea area b) Heterotrophic nearshore area. Control (C) corresponds to the response variable value in PAR treatment; UV corresponds to the value in the UV treatment; 'Additive effect' is the sum of control value plus the single UV and Dust effects, and UVD is the response-variable value in the UVD treatment. The strength of interactive effect represents the quotient between the UVD and Control treatments. A: antagonistic interaction; S: synergistic interaction. The sign of the types of interactive effects and calculations are based on Piggott et al. (2015) (see Material and Methods section). Particulate primary production (PP_P), excreted organic carbon by phytoplankton (EOC), bacterial respiration (BR), heterotrophic bacterial production (HBP), bacterial growth efficiency (BGE), and bacterial carbon demand: excreted organic carbon (BCD:EOC) ratio.

Treatment	PP_P	EOC	BR	HBP	BGE	BCD:EOC
Autotrophic open sea area						
C	7.34	24.19	36.05	7.67	0.18	1.91
UV	10.76	30.00	39.39	7.19	0.16	1.59
D	8.47	36.75	25.71	6.44	0.21	0.95
Additive effect	11.89	42.55	29.05	5.96	0.19	0.62
UVD	5.60	15.33	33.13	13.59	0.29	4.02
Interaction type	S-	S-	A-	S+	A-	S+
Relative strength	0.76	0.63	0.92	1.77	1.61	2.10
Biological meaning	Inhibition	Inhibition	Stimulation	Stimulation	Stimulation	Uncoupling
Heterotrophic nearshore area						
C	4.55	15.54	41.76	4.84	0.11	3.89
UV	6.17	25.46	46.95	6.56	0.20	2.83
D	4.02	22.06	39.67	9.79	0.20	0.45
Additive effect	5.63	31.97	44.86	11.51	0.29	0.42
UVD	4.89	15.85	50.16	8.35	0.15	0.32
Interaction type	A+	A+	S+	A+	A+	S-
Relative strength	1.08	1.02	1.20	1.72	1.35	0.08
Biological meaning	Stimulation	Stimulation	Stimulation	Inhibition	Stimulation	Coupling

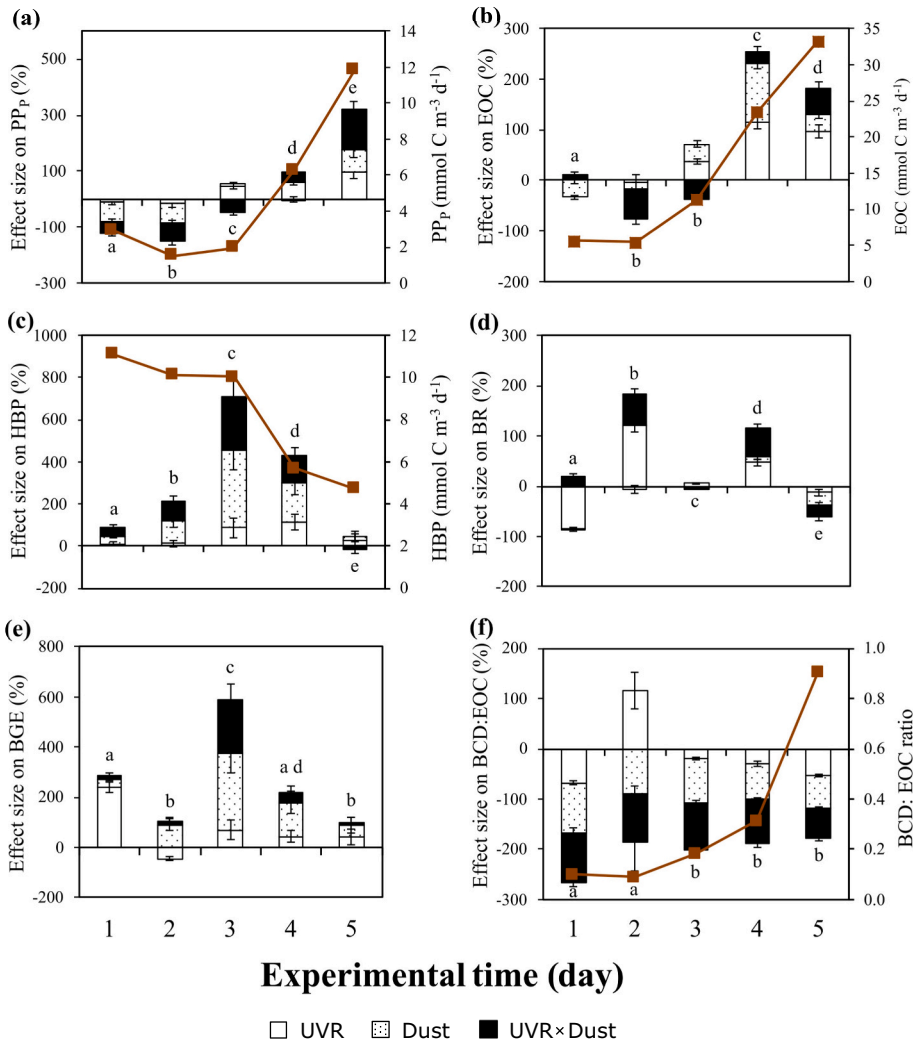

Fig. 4. The effect size of UVR, Dust, and UVR × Dust on metabolic variables from the heterotrophic nearshore area. Figure includes (a) particulate primary production (PP_P), (b) excretion of organic carbon by phytoplankton (EOC), (c) heterotrophic bacterial production (HBP), (d) bacterial respiration (BR), (e) bacterial growth efficiency (BGE) and (f) bacterial carbon demand: excretion of organic carbon (BCD: EOC) ratio. Each segment in a stacked bar represents the mean values of three replicates, while the vertical lines indicate the standard deviation for each factor UVR, Dust, and UVR × Dust. The letters indicate differences among UVR × Dust treatment by LSD post hoc test over the experiment. The brown line links mean values of the corresponding variable under UVR × Dust treatment.

particularly in D and UVD decreased below 1 from the first day to the end of the incubation (Fig. A6f, UVR × Dust×Time $p < 0.05$, Table A2a), and hence, EOC satisfied 100 % of the C required by heterotrophic bacterial metabolism in both treatments with dust addition. The single effect sizes of UVR and Dust on BCD: EOC were mostly negative (except the effect size of UVR at day 2). The effect size of UVR × Dust on BCD: EOC ratio also was negative and similar in magnitude to individual Dust effect size (Fig. 4f) suggesting that Dust was the main factor coupling the phytoplankton-bacteria interaction.

Finally, the Chl *a* concentration (as a proxy of phytoplankton biomass) increased in all treatments, reaching its highest values in the D treatment at the end of the experiment whereas the BA increased during the first three days of the experiment up to 4-fold in both Dust treatments (Fig. A5b,d; Table A2b).

From the BCD:EOC ratio values obtained in the experimental study we evaluated the potential variation of the BCD:EOC vs. PPT:CR relationship under a future global change scenario of Dust inputs under UVR in the Alboran Sea (shown in Fig. 5).

To do this, the mean effect size (ES) of UVR × Dust on BCD:EOC ratio (−0.87 for heterotrophic nearshore area, and 1.15 for autotrophic open sea) obtained from each experiment was used to project the future field values for each station according to its metabolism (i.e., W-uncoupled or S-uncoupled sites, Table A1a) following the expression:

$$\text{Future ratio} = \text{current ratio} + (\text{current ratio} \times \text{ES}).$$

Then we applied the empirical model of the current relationship between BCD:EOC and PP_T:CR built from our observational study (Fig. 2e).

Fig. 5 shows that the combined effect of UVR and Dust on BCD:EOC ratio in the strongly uncoupled stations will couple phytoplankton-bacteria interaction and potentially deviate the metabolic balance toward autotrophy (PP_T:CR > 1). By contrast, in the weakly uncoupled stations, the combined UVR × Dust effect will strengthen the uncoupling degree with a potential decrease in the PPT:CR ratio.

4. Discussion

4.1. Field study

This study fills a gap of knowledge concerning how the C flux between phytoplankton (via excretion of organic carbon) and heterotrophic bacteria (via bacterial carbon demand) are controlled by the interaction of two major environmental stressors under future global change scenarios. This topic is timely because global-change-driven

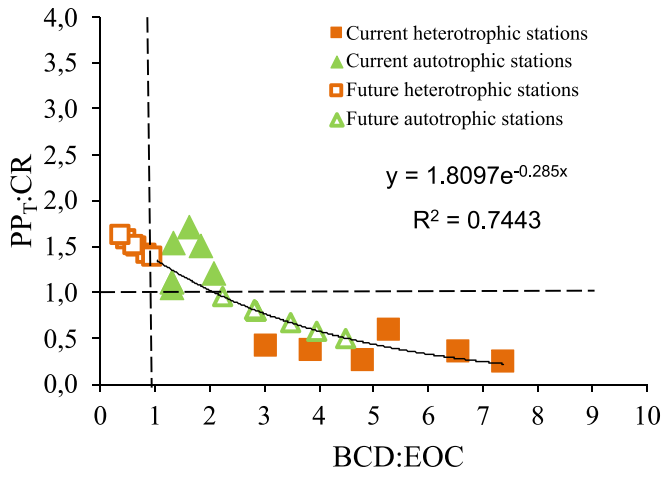

Fig. 5. Phytoplankton: Bacteria commensalistic interaction (BCD: EOC) exponentially relates to the metabolic balance PP_T: CR in the south-western Mediterranean Sea (solid symbols). Future joint Saharan dust and ultraviolet radiation (UVR) promote the coupling (BCD: EOC <1) in heterotrophic nearshore areas whereas enhanced the uncoupling (BCD: EOC >1) in autotrophic open-sea areas, and generalized increase in metabolic balance (PP_T: CR) in both areas, broke the BCD: EOC vs. PP_T: CR exponential relation.

alterations in these fluxes have consequences for the C sequestration via microbial loop in marine ecosystems (Jiao et al., 2014). With this focus, we first established the current state of the phytoplankton-bacteria commensalistic interaction over SW Mediterranean, resulting in an uncoupled relationship (i.e., BCD was not satisfied by EOC). However, the high values of uncoupling could be somewhat biased, as the measured EOC rates represent the net values of C released, given that bacterial respiration was not impeded during the incubation. Besides, we found a significant negative exponential regression between the degree of uncoupling (BCD:EOC) and the metabolic balance of the ecosystem (PP_T:CR ratio) in the field study. This finding underlines the key role that this trophic interaction, at the base of food web, plays in modulating the function of oligotrophic marine areas as net C-sink or C-source. Our empirical evidence complements the insight by González-Benítez et al. (2019) since the link between EOC and BCD could predict the metabolic balance of the ecosystem (Fig. 2e) in metabolically diverse marine ecosystems (sensu stricto Serret et al., 2015). Therefore, we propose that the BCD:EOC ratio may be a predictor to understand whether the net outgassing of CO_2 is the prevalent process in the ecosystem or, on the contrary, C-sequestration is, as was suggested by Hoppe et al. (2002). The above-outlined consideration strongly underlies our approach, that directly quantified (i) the EOC by phytoplankton, (ii) the BR and CR rates and (iii) the HBP and BGE, all these variables being measured under identical (natural or experimental) and realistic conditions. The challenge of measuring both BR and CR simultaneously is not exempt of some uncertainty, as filtering by GF/F may result in a slight underestimation of BR, because not the entire fraction could pass through the filter.

The spatial patterns of the BCD:EOC matched with those arising from the metabolic balance, that is, weakly uncoupled stations were net autotrophic (named autotrophic open-sea area), while strongly uncoupled stations were net heterotrophic (named heterotrophic nearshore area). This contrasting trend may be due to the stronger influence of allochthonous DOC in areas near the continental shelf which would support high community respiration (Gazeau et al., 2005), although the surface circulation could also play a key role in DOC transport (Santinelli et al., 2021).

Likewise, our findings agree with the general pattern established for open-sea areas, where HBP and EOC are often linked (i.e., positively correlated) in unproductive oligotrophic waters such as Antarctic offshore waters (Morán et al., 2001) or the Celtic Sea (García-Martín et al., 2019). By contrast, such linkage is absent in coastal waters (NE Atlantic coastal system, Morán et al., 2002), eutrophic waters (Baines and Pace, 1991), upwelling areas (Teira et al., 2015), estuarine systems (Morán et al., 2013) or the western North Atlantic (Baetge et al., 2021).

Two non-exclusive mechanisms underpin this contrasting pattern. First, the higher %EOC in autotrophic open sea area compared to heterotrophic nearshore stations may be related to a higher degree of uncoupling between photosynthesis and growth due to UVR (Berman-Frank and Dubinsky, 1999). Thus, %EOC could be an indicator of lesser algal viability (Carrillo et al., 2002; González-Olalla et al., 2017). Others potential explanations did not elucidate this result, as the degree of P limitation was lower in the autotrophic open area than in the heterotrophic nearshore area (González-Olalla et al., 2017).

Second, BGE was slightly higher in autotrophic open sea stations than in heterotrophic nearshore stations, related to the bacterial use of EOC. The C released by algae is the preferred C-source for heterotrophic bacteria because it is mainly composed of low-molecular-weight compounds readily assimilable by bacteria (Kritzberg et al., 2005, 2006).

One plausible explanation for the divergent results concerning the dust and UVR impacts could be related to differential P-limitation (TDN: TDP ratio and sestonic C: P ratio) in both areas. This was higher in the heterotrophic nearshore than in the autotrophic open-sea areas (González-Olalla et al., 2017) These differences in the abiotic environment could condition both the physiology, metabolic status, and BCD: EOC ratio of the microbial communities.

4.2. *Experimental study*

The second step in the present study was to test experimentally how two contrasting marine areas (i.e., heterotrophic nearshore and autotrophic open sea) could be affected under future scenarios of dust inputs and high UVR exposure. In agreement with our hypothesis, we found an opposite response to both environmental drivers (UVR and Dust) of autotrophic (PP_P, EOC, Chl *a*), heterotrophic variables (HBP, BR, BGE, HBA), and the BCD:EOC ratio, depending on area.

In the autotrophic open sea, phytoplankton underwent damage by UVR × Dust suggesting its high sensitivity to both drivers (negative synergetic effect), whereas BGE and HBP were higher, and bacteria strongly grew, under UVR × Dust conditions (Figs. A4, A5). This bacterial response suggests a competitive advantage of heterotrophic bacteria compared to phytoplankton in leveraging the Saharan dust-derived nutrients (Gazeau et al., 2021b). The above responses determined that the BCD:EOC ratio increased, and consequently that C-flux inside the microbial loop shifted toward a greater uncoupling (i.e., EOC did not satisfy BCD). A more uncoupled phytoplankton-bacteria relationship along with a greater bacterial growth, indicate that other C sources could satisfy bacterial demands, such as DOC transported by Saharan dust (Galletti et al., 2020) or DOC derived by cellular death due to the harmful UVR effect on autotrophic community (González-Olalla et al., 2017).

In the heterotrophic nearshore area, PP_P, EOC, and Chl *a* were strongly stimulated (positive antagonistic effect) whereas HBP, BGE, and BA decreased under UVR × Dust conditions over the experiment resulting in BCD:EOC ratio < 1 (i.e., EOC was enough to satisfy BCD). These contrasting responses of phytoplankton and bacteria to UVR and Dust suggest a competitive advantage of the phytoplankton by the inorganic nutrients linked to dust in these waters, as we discarded a substantial alteration of the metabolic balance by potential mesozooplankton grazing and respiration in this experimental condition (see Fig. S4 in Cabrerizo et al., 2016). These results support our hypothesis and are in line with previous findings on the Alboran Sea which will behave as C sink under future UVR × Dust conditions (Cabrerizo et al., 2016).

5. Conclusion

Greater dust pulses derived from higher frequency and intensity of dust exportation events from the Sahara (Cabrerizo et al., 2021; Martino et al., 2014), together with higher UVR fluxes in the upper layers may induce significant changes in the C flux through the phytoplankton-bacteria link in marine oligotrophic ecosystems as projected in Fig. 5. Although caution should be exercised in extrapolating results from a small oceanic area, such as the Alborán Sea, to the entire Mediterranean Sea basin (or even other oligotrophic areas/basins), our results point out a clear diverting trend of the phytoplankton-bacteria coupling under changing environmental conditions. Ocean-scale models predict an expansion of LNLC areas in a future warmer, stratified, UVR-stressed ocean, along with step increases in regional dust emission due to more severe desertification, which could affect the C-flux ways and biomass of microbial communities on the future marine ecosystems.

CRediT authorship contribution statement

Presentación Carrillo: Writing – review & editing, Writing – original draft, Visualization, Validation, Supervision, Project administration, Methodology, Investigation, Funding acquisition, Formal analysis, Data curation, Conceptualization. **Juan Manuel González-Olalla:** Writing – review & editing, Visualization, Validation, Supervision, Methodology, Investigation. **Marco J. Cabrerizo:** Writing – review & editing, Visualization, Validation, Supervision, Methodology, Investigation. **Manuel Villar-Argaiz:** Writing – review & editing, Methodology, Investigation. **Juan Manuel Medina-Sánchez:** Writing – review & editing, Visualization, Validation, Supervision, Project administration, Investigation, Funding acquisition, Conceptualization, Methodology.

Declaration of competing interest

The authors declare that they have no known competing financial interests or personal relationships that could have appeared to influence the work reported in this paper.

Data availability

Data will be made available on request.

Acknowledgements

This work was funded by Ministerio de Economía y Competitividad and Fondo Europeo de Desarrollo Regional (FEDER) (METAS Project, CGL2015-67682-R to PC and JMMS), Ministerio de Ciencia e Innovación and by the European NextGenerationEU/PRTR (TED2021-131262B-I00 to JMM-S and PC), and Campus de Excelencia Internacional del Mar (CeiMar, CEIJ-008 to MJC). JMG-O was supported by Ministerio de Ciencia e Innovacion and European Union - Next Generation through the project TED2021-131262B-I00. MJC was supported by Captación, Incorporación y Movilidad de Capital Humano de I + D + i postdoctoral contract from Junta de Andalucía (POSTDOC-21-00044).

We are deeply grateful to E. Corral for the help during the experiments aboard, and to J. M. Mercado for providing us with the CTD device. We thank David Nesbitt for the English writing assistance. We are also indebted to all the crew of BO Fco. de Paula Navarro for support during the MICROSENS campaign.

Appendix A. Supplementary data

Supplementary data to this article can be found online at https://doi.org/10.1016/j.scitotenv.2024.172220.

References

APHA, 2017. Standard Methods for the Examination of Water and Wastewater American Public Health Association. American Public Health Association, Washington.

Baetge, N., Behrenfeld, M.J., Fox, J., Halsey, K.H., Mojica, K.D.A., Novoa, A., Stephens, B.M., Carlson, C.A., 2021. The seasonal flux and fate of dissolved organic carbon through bacterioplankton in the Western North Atlantic. Front. Microbiol. 12 https://doi.org/10.3389/fmicb.2021.669883.

Baines, S.B., Pace, M.L., 1991. The production of dissolved organic matter by phytoplankton and its importance to bacteria: patterns across marine and freshwater systems. Limnol. Oceanogr. 36, 1078–1090. https://doi.org/10.4319/LO.1991.36.6.1078.

Behrenfeld, M.J., O'Malley, R.T., Siegel, D.A., McClain, C.R., Sarmiento, J.L., Feldman, G.C., Milligan, A.J., Falkowski, P.G., Letelier, R.M., Boss, E.S., 2006. Climate-driven trends in contemporary ocean productivity. Nature 444, 752–755. https://doi.org/10.1038/nature05317.

Bell, R.T., 1983. Estimating production of heterotrophic bacterioplankton via incorporation of tritiated thymidine. In: Kemp, P.F., Sherr, B.F., Cole, J.J. (Eds.), Handbook of Methods in Aquatic Microbial Ecology. Lewis Publishers, Boca Ratón, Florida, USA, pp. 495–503.

Berman-Frank, I., Dubinsky, Z., 1999. Balanced growth in aquatic plants: myth or reality? Phytoplankton use the imbalance between carbon assimilation and biomass production to their strategic advantage. Bioscience 49, 29–37. https://doi.org/10.1525/bisi.1999.49.1.29.

Borchardt, T., Fisher, K.v., Ebling, A.M., Westrich, J.R., Xian, P., Holmes, C.D., Landing, W.M., Lipp, E.K., Wetz, M.S., Ottesen, E.A., 2020. Saharan dust deposition initiates successional patterns among marine microbes in the Western Atlantic. Limnol. Oceanogr. 65, 191–203. https://doi.org/10.1002/lno.11291.

Cabrerizo, M.J., Medina-Sánchez, J.M., González-Olalla, J.M., Villar-Argaiz, M., Carrillo, P., 2016. Saharan dust inputs and high UVR levels jointly alter the metabolic balance of marine oligotrophic ecosystems. Sci. Rep. 6 https://doi.org/10.1038/srep35892.

Cabrerizo, M.J., Medina-Sánchez, J.M., González-Olalla, J.M., Sánchez-Gómez, D., Carrillo, P., 2021. Microbial plankton responses to multiple environmental drivers in marine ecosystems with different phosphorus limitation degrees. Sci. Total Environ. 151491 https://doi.org/10.1016/j.scitotenv.2021.151491.

Calvin, K., Dasgupta, D., Krinner, G., Mukherji, A., Thorne, P.W., Trisos, C., Romero, J., Aldunce, P., Barrett, K., Blanco, G., Cheung, W.W.L., Connors, S., Denton, F., Diongue-Niang, A., Dodman, D., Garschagen, M., Geden, O., Hayward, B., Jones, C., Jotzo, F., Krug, T., Lasco, R., Lee, Y.-Y., Masson-Delmotte, V., Meinshausen, M., Mintenbeck, K., Mokssit, A., Otto, F.E.L., Pathak, M., Pirani, A., Poloczanska, E., Pörtner, H.-O., Revi, A., Roberts, D.C., Roy, J., Ruane, A.C., Skea, J., Shukla, P.R., Slade, R., Slangen, A., Sokona, Y., Sörensson, A.A., Tignor, M., van Vuuren, D., Wei, Y.-M., Winkler, H., Zhai, P., Zommers, Z., Hourcade, J.-C., Johnson, F.X., Pachauri, S., Simpson, N.P., Singh, C., Thomas, A., Totin, E., Alegría, A., Armour, K., Bednar-Friedl, B., Blok, K., Cissé, G., Dentener, F., Eriksen, S., Fischer, E., Garner, G., Guivarch, C., Haasnoot, M., Hansen, G., Hauser, M., Hawkins, E., Hermans, T., Kopp, R., Leprince-Ringuet, N., Lewis, J., Ley, D., Ludden, C., Niamir, L., Nicholls, Z., Some, S., Szopa, S., Trewin, B., van der Wijst, K.-I., Winter, G., Witting, M., Birt, A., Ha, M., 2023. IPCC, 2023: Climate Change 2023: Synthesis Report. Contribution of Working Groups I, II and III to the Sixth Assessment Report of the Intergovernmental Panel on Climate Change [Core Writing Team, H. Lee and J. Romero (eds.)]. IPCC, Geneva, Switzerland. https://doi.org/10.59327/IPCC/AR6-9789291691647.

Carrillo, P., Medina-Sánchez, J.M., Villar-Argaiz, M., 2002. The interaction of phytoplankton and bacteria in a high mountain lake: importance of the spectral composition of solar radiation. Limnol. Oceanogr. 47, 1294–1306. https://doi.org/10.4319/lo.2002.47.5.1294.

Carrillo, P., Medina-Sánchez, J.M., Durán, C., Herrera, G., Villafañe, V.E., Helbling, E.W., 2015a. Synergistic effects of UVR and simulated stratification on commensalistic phytoplankton–bacteria relationship in two optically contrasting oligotrophic Mediterranean lakes. Biogeosciences 12, 697–712. https://doi.org/10.5194/bg-12-697-2015.

Carrillo, P., Medina-Sánchez, J.M., Herrera, G., Durán, C., Segovia, M., Cortés, D., Salles, S., Korbee, N., Figueroa, F., Mercado, J.M., 2015b. Interactive effect of UVR and phosphorus on the coastal phytoplankton community of the western mediterranean sea: unravelling eco-physiological mechanisms. PLoS One 10. https://doi.org/10.1371/journal.pone.0142987.

Céa, B., Lefèvre, D., Chirurgien, L., Raimbault, P., Garcia, N., Charrière, B., Grégori, G., Ghiglione, J.F., Barani, A., Lafont, M., van Wambeke, F., 2015. An annual survey of bacterial production, respiration and ectoenzyme activity in coastal NW Mediterranean waters: temperature and resource controls. Environ. Sci. Pollut. Res. 22, 13654–13668. https://doi.org/10.1007/S11356-014-3500-9.

Cerro, J.C., Cerdà, V., Caballero, S., Bujosa, C., Alastuey, A., Querol, X., Pey, J., 2020. Chemistry of dry and wet atmospheric deposition over the Balearic Islands, NW Mediterranean: source apportionment and African dust areas. Sci. Total Environ. 747, 141187.

Cirri, E., Pohnert, G., 2019. Algae−bacteria interactions that balance the planktonic microbiome. New Phytol. 23, 100–106. https://doi.org/10.1111/nph.15765.

Chien, C.-te, Mackey, K.R.M., Dutkiewicz, S., Mahowald, N.M., Prospero, J.M., Paytan, A., 2016. Effects of African dust deposition on phytoplankton in the western tropical Atlantic Ocean off Barbados. Glob. Biogeochem. Cycles 30, 716–734. https://doi.org/10.1002/2015GB005334.

del Giorgio, P.A., Cole, J.J., 1998. Bacterial growth efficiency in natural aquatic systems. Annu. Rev. Ecol. Syst. 29, 503–544.

Desboeufs, K., Fu, F., Bressac, M., Tovar-Sánchez, A., Triquet, S., Doussin, J.-F., Giorio, C., Chazette, P., Disnaquet, J., Feron, A., Formenti, P., Maisonneuve, F.,

Rodríguez-Romero, A., Zapf, P., Dulac, F., Guieu, C., 2021. Wet deposition in the remote western and Central Mediterranean as a source of trace metals to surface seawater. Atmos. Chem. Phys. Discuss 1–41. https://doi.org/10.5194/acp-2021-624.

Djaoudi, K., van Wambeke, F., Barani, A., Hélias Nunige, S., Sempere, R., Pulido-Villena, E., Wambeke, V., 2018. Atmospheric fluxes of soluble organic C, N, and P to the Mediterranean Sea: potential biogeochemical implications in the surface layer atmospheric fluxes of soluble organic C, N, and P to the Mediterranean Sea: potential biogeochemical implications in the 2 surface layer. Prog. Oceanogr. 163, 59–69. https://doi.org/10.1016/j.pocean.2017.07.008i.

Durrieu de Madron, X., Guieu, C., Sempéré, R., Conan, P., Cossa, D., D'Ortenzio, F., Estournel, C., Gazeau, F., Rabouille, C., Stemmann, L., Bonnet, S., Diaz, F., Koubbi, P., Radakovitch, O., Babin, M., Baklouti, M., Bancon-Montigny, C., Belviso, S., Bensoussan, N., Bonsang, B., Bouloubassi, I., Brunet, C., Cadiou, J.F., Carlotti, F., Chami, M., Charmasson, S., Charrière, B., Dachs, J., Doxaran, D., Dutay, J.C., Elbaz-Poulichet, F., Eléaume, M., Eyrolles, F., Fernandez, C., Fowler, S., Francour, P., Gaertner, J.C., Galzin, R., Gasparini, S., Ghiglione, J.F., Gonzalez, J.L., Goyet, C., Guidi, L., Guizien, K., Heimbürger, L.E., Jacquet, S.H.M., Jeffrey, W.H., Joux, F., le Hir, P., Leblanc, K., Lefèvre, D., Lejeusne, C., Lemé, R., Loÿe-Pilot, M.D., Mallet, M., Méjanelle, L., Mélin, F., Mellon, C., Mérigot, B., Merle, P.L., Migon, C., Miller, W.L., Mortier, L., Mostajir, B., Mousseau, L., Moutin, T., Para, J., Pérez, T., Petrenko, A., Poggiale, J.C., Prieur, L., Pujo-Pay, M., Pulido-Villena, Raimbault, P., Rees, A.P., Ridame, C., Rontani, J.F., Ruiz Pino, D., Sicre, M.A., Taillandier, V., Tamburini, C., Tanaka, T., Taupier-Letage, I., Tedetti, M., Testor, P., Thébault, H., Thouvenin, B., Touratier, F., Tronczynski, J., Ulses, C., van Wambeke, F., Vantrepotte, V., Vaz, S., Verney, R., 2011. Marine ecosystems' responses to climatic and anthropogenic forcings in the Mediterranean. Prog. Oceanogr. 91, 97–166. https://doi.org/10.1016/J.POCEAN.2011.02.003.

Galic, N., Sullivan, L.L., Grimm, V., Forbes, V.E., 2018. When things don't add up: quantifying impacts of multiple stressors from individual metabolism to ecosystem processing. Ecol. Lett. 21, 568–577. https://doi.org/10.1111/ele.12923.

Galletti, Y., Becagli, S., di Sarra, A., Gonnelli, M., Pulido-Villena, E., Sferlazzo, D.M., Traversi, R., Vestri, S., Santinelli, C., 2020. Atmospheric deposition of organic matter at a remote site in the Central Mediterranean Sea: implications for the marine ecosystem. Biogeosciences 17, 3669–3684. https://doi.org/10.5194/bg-17-3669-2020.

Gao, K., Helbling, E.W., Häder, D.P., Hutchins, D.A., 2012. Responses of marine primary producers to interactions between ocean acidification, solar radiation, and warming. Mar. Ecol. Prog. Ser. 470, 167–189. https://doi.org/10.3354/MEPS10043.

García-Martín, E.E., Daniels, C.J., Davidson, K., Davis, C.E., Mahaffey, C., Mayers, K.M. J., McNeill, S., Poulton, A.J., Purdie, D.A., Tarran, G.A., Robinson, C., 2019. Seasonal changes in plankton respiration and bacterial metabolism in a temperate shelf sea. Prog. Oceanogr. 177 https://doi.org/10.1016/j.pocean.2017.12.002.

Gazeau, F., Duarte, C.M., Gattuso, J.-P., Barrón, C., Navarro, N., Ruiz, S., Prairie, Y.T., Calleja, M., Delille, B., Frankignoulle, M., Borges, A.v, 2005. Whole-system metabolism and CO2 fluxes in a Mediterranean Bay dominated by seagrass beds (Palma Bay, NW Mediterranean). Biogeosciences 2, 43–60. https://doi.org/10.5194/BG-2-43-2005.

Gazeau, F., van Wambeke, F., Marañón, E., Pérez-Lorenzo, M., Alliouane, S., Stolpe, C., Blasco, T., Leblond, N., Zäncker, B., Engel, A., Marie, B., Dinasquet, J., Guieu, C., 2021a. Impact of dust addition on the metabolism of Mediterranean plankton communities and carbon export under present and future conditions of pH and temperature. Biogeosci. Discuss. 1–74 https://doi.org/10.5194/bg-2021-20.

Gazeau, F., Ridame, C., Van Wambeke, F., Alliouane, S., Stolpe, C., Irisson, J.-O., Marro, S., Grisoni, J.-M., De Liège, G., Nunige, S., Djaoudi, K., Pulido-Villena, E., Dinasquet, J., Obernosterer, I., Catala, P., Guieu, C., 2021b. Impact of dust addition on Mediterranean plankton communities under present and future conditions of pH and temperature: an experimental overview. Biogeosciences 18, 5011–5034. https://doi.org/10.5194/bg-18-5011-2021.

Geisen, C., Ridame, C., Journet, E., Delmelle, P., Marie, D., Monaco, C. lo, Metzl, N., Ammar, R., Kombo, J., Cardinal, D., 2021. Phytoplanktonic response to simulated volcanic and desert dust deposition events in the south Indian and southern oceans. Glob. Biogeochem. Cy. https://doi.org/10.1002/ESSOAR.10507198.2.

González-Benítez, N., García-Corral, L.S., Morán, X.A.G., Middelburg, J.J., Pizay, M.D., Gattuso, J.P., 2019. Drivers of microbial carbon fluxes variability in two oligotrophic mediterranean coastal systems. Sci. Rep. 9 https://doi.org/10.1038/s41598-019-53650-z.

González-Olalla, J.M., Medina-Sánchez, J.M., Cabrerizo, M.J., Villar-Argáiz, M., Sánchez-Castillo, P.M., Carrillo, P., 2017. Contrasting effect of Saharan dust and UVR on autotrophic picoplankton in nearshore versus offshore waters of Mediterranean Sea. Eur. J. Vasc. Endovasc. Surg. 122, 2085–2103. https://doi.org/10.1002/2017JG003834.

González-Olalla, J.M., Powell, J.A., Brahney, J., 2024. Dust storms increase the tolerance of phytoplankton to thermal and pH changes. Glob. Chang. Biol. 30, e17055 https://doi.org/10.1111/gcb.17055.

Gunderson, A.R., Armstrong, E.J., Stillman, J.H., 2016. Multiple stressors in a changing world: the need for an improved perspective on physiological responses to the dynamic marine environment. Annu. Rev. Mar. Sci. 8, 357–378. https://doi.org/10.1146/annurev-marine-122414-033953.

Guo, C., Xia, X., Pitta, P., Herut, B., Rahav, E., Berman-Frank, I., Giannakourou, A., Tsiola, A., Tsagaraki, T.M., Liu, H., 2016. Shifts in microbial community structure and activity in the ultra-oligotrophic eastern mediterranean sea driven by the deposition of saharan dust and European aerosols. Front. Mar. Sci. 3, 170. https://doi.org/10.3389/FMARS.2016.00170/BIBTEX.

Hamilton, D.S., Perron, M.M.G., Bond, T.C., Bowie, A.R., Buchholz, R.R., Guieu, C., Ito, A., Maenhaut, W., Myriokefalitakis, S., Olgun, N., Rathod, S.D., Schepanski, K., Tagliabue, A., Wagner, R., Mahowald, N.M., 2022. Earth, wind, fire, and pollution. Aerosol Nutrient Sources and Impacts on Ocean Biogeochemistry. Ann. Rev. Mar. Sci. 14 https://doi.org/10.1146/annurev-marine-031921, 11.1-11.28.

Hewitt, J.E., Thrush, S.F., Dayton, P.K., Bonsdorff, E., 2007. The effect of spatial and temporal heterogeneity on the design and analysis of empirical studies of scale-dependent systems. Am. Nat. 169, 398–408. https://doi.org/10.1086/510925.

Hoppe, H.G., Gocke, K., Koppe, R., Begler, C., 2002. Bacterial growth and primary production along a north–south transect of the Atlantic Ocean. Nature 416, 168–171. https://doi.org/10.1038/416168a.

IPCC, 2021. IPCC, 2021: Climate Change 2021: The Physical Science Basis. Contribution of Working Group I to the Sixth Assessment Report of the Intergovernmental Panel on Climate Change. Cambridge University Press, Cambridge, United Kingdom and New York.

Jeffrey, S.W., Humphrey, G.F., 1975. New spectrophotometric equations for determining chlorophylls a, b, c 1, and c 2 in higher plants, algae, and natural phytoplankton. Biochem. Physiol. Pflanz. 167, 191–194.

Jiao, N., Robinson, C., Azam, F., Thomas, H., Baltar, F., Dang, H., Hardman-Mountford, N.J., Johnson, M., Kirchman, D.L., Koch, B.P., Legendre, L., Li, C., Liu, J., Luo, T., Luo, Y.W., Mitra, A., Romanou, A., Tang, K., Wang, X., Zhang, C., Zhang, R., 2014. Mechanisms of microbial carbon sequestration in the ocean – future research directions. Biogeosciences 11, 5285–5306. https://doi.org/10.5194/bg-11-5285-2014.

Jickells, T., Moore, C.M., 2015. The importance of atmospheric deposition for ocean productivity. Annu. Rev. Ecol. Evol. Syst. 46, 481–501. https://doi.org/10.1146/ANNUREV-ECOLSYS-112414-054118.

Koroleff, O., 1977. Simultaneous persulfate oxidation of phosphorus and nitrogen compounds in water. In: Grasshoff, K. (Ed.), Report on the Baltic Intercalibration Workshop. Compiler, Kiel, Germany, pp. 52–53.

Kritzberg, E.S., Cole, J.J., Pace, M.M., Granéli, W., 2005. Does autochthonous primary production drive variability in bacterial metabolism and growth efficiency in lakes dominated by terrestrial C inputs? Aquat. Microb. Ecol. 38, 103–111. https://doi.org/10.3354/AME038103.

Kritzberg, E.S., Cole, J.J., Pace, M.M., Granéli, W., 2006. Bacterial growth on Allochthonous carbon in humic and Nutrient-Enriched Lakes: results from whole-Lake 13C addition experiments. Ecosystems 9, 489–499. https://doi.org/10.1007/s10021-005-0115-5.

Kwiatkowski, L., Torres, O., Bopp, L., Aumont, O., Chamberlain, M.R., Christian, J.P., Dunne, J., Gehlen, M., Ilyina, T.G., John, J., Lenton, A., Li, H.S., Lovenduski, N.C., Orr, J., Palmieri, J., Santana-Falcón, Y., Schwinger, J., Séférian, R.A., Stock, C., Tagliabue, A., Takano, Y., Tjiputra, J., Toyama, K., Tsujino, H., Watanabe, M., Yamamoto, A., Yool, A., Ziehn, T., 2020. Twenty-first century ocean warming, acidification, deoxygenation, and upper-ocean nutrient and primary production decline from CMIP6 model projections. Biogeosciences 17, 3439–3470. https://doi.org/10.5194/BG-17-3439-2020.

Lagaria, A., Mandalakis, M., Mara, P., Papageorgiou, N., Pitta, P., Tsiola, A., Kagiorgi, M., Psarra, S., 2017. Phytoplankton response to Saharan dust depositions in the eastern Mediterranean Sea: a mesocosm study. Front. Mar. Sci. 3, 00287. https://doi.org/10.3389/FMARS.2016.00287.

Lee, S., Fuhrman, J.A., 1987. Relationships between biovolume and biomass of naturally derived marine bacterioplankton. Appl. Environ. Microbiol. 53, 1298–1303. https://doi.org/10.1128/AEM.53.6.1298-1303.1987.

Lekunberri, I., Lefort, T., Romero, E., Vázquez-Domínguez, E., Romera-Castillo, C., Marrasé, C., Peters, F., Weinbauer, M., Gasol, J.M., 2010. Effects of a dust deposition event on coastal marine microbial abundance and activity, bacterial community structure and ecosystem function. J. Plankton Res. 32, 381–396. https://doi.org/10.1093/PLANKT/FBP137.

López-Sandoval, D.C., Fernández, A., Marañón, E., 2011. Dissolved and particulate primary production along a longitudinal gradient in the Mediterranean Sea. Biogeosciences 8, 815–825. https://doi.org/10.5194/bg-8-815-2011.

Maki, T., Lee, K.C., Pointing, S.B., Watanabe, K., Aoki, K., Archer, S.D.J., Lacap-Bugler, D.C., Ishikawa, A., 2021. Desert and anthropogenic mixing dust deposition influences microbial communities in surface waters of the western Pacific Ocean. Sci. Total Environ. 791 https://doi.org/10.1016/J.SCITOTENV.2021.148026.

Marañón, E., Cermeño, P., Fernández, E., Rodríguez, J., Zabala, L., 2004. Significance and mechanisms of photosynthetic production of dissolved organic carbon in a coastal eutrophic ecosystem. Limnol. Oceanogr. 49, 1652–1666. https://doi.org/10.4319/LO.2004.49.5.1652.

Marañón, E., Cermeño, P., Pérez, V., 2005. Continuity in the photosynthetic production of dissolved organic carbon from eutrophic to oligotrophic waters. Mar. Ecol. Prog. Ser. 299, 7–17. https://doi.org/10.3354/MEPS299007.

Marañón, E., Fernández, A., Mourino-Carballido, B., MartÍnez-GarcÍa, S., Teira, E., Cermeno, P., Chouciño, P., Huete-Ortega, M., Fernández, E., Calvo-Diaz, A., Moran, X.A.G., Bode, A., Moreno-Ostos, E., Varela, M.M., Patey, M.D., Achterberg, E. P., 2010. Degree of oligotrophy controls the response of microbial plankton to Saharan dust. Limnol. Oceanogr. 55 (6), 2339–2352.

Marañón, E., van Wambeke, F., Uitz, J., Boss, E.S., DImier, C., DInasquet, J., Engel, A., Haëntjens, N., Perez-Lorenzo, M., Taillandier, V., Zäncker, B., 2021. Deep maxima of phytoplankton biomass, primary production and bacterial production in the Mediterranean Sea. Biogeosciences 18, 1749–1767. https://doi.org/10.5194/BG-18-1749-2021.

Martino, M., Hamilton, D., Baker, A.R., Jickells, T.D., Bromley, T., Nojiri, Y., Quack, B., Boyd, P.W., 2014. Western Pacific atmospheric nutrient deposition fluxes, their impact on surface ocean productivity. Glob. Biogeochem. Cy. 28, 712–728. https://doi.org/10.1002/2013GB004794.

Meador, T.B., Gogou, A., Spyres, G., Herndl, G.J., Krasakopoulou, E., Psarra, S., Yokokawa, T., de Corte, D., Zervakis, V., Repeta, D.J., 2010. Biogeochemical

relationships between ultrafiltered dissolved organic matter and picoplankton activity in the eastern Mediterranean Sea. Deep Sea Res. Pt II: Top. Stud. Oceanogr. 57, 1460–1477. https://doi.org/10.1016/J.DSR2.2010.02.015.

Medina-Sánchez, J.M., Herrera, G., Durán, C., Villar-Argaiz, M., Carrillo, P., 2017. Optode use to evaluate microbial planktonic respiration in oligotrophic ecosystems as an indicator of environmental stress. Aquat. Sci. 79, 529–541. https://doi.org/10.1007/s00027-016-0515-y.

Moore, J.K., Fu, W., Primeau, F., Britten, G.L., Lindsay, K., Long, M., Doney, S.C., Mahowald, N., Hoffman, F., Randerson, J.T., 2018. Sustained climate warming drives declining marine biological productivity. Science 1979 (359), 1139–1143. https://doi.org/10.1126/science.aao6379.

Morán, X.A., Gasol, J.M., Pedrós- Alió, C., Estrada, M., 2001. Dissolved and particulate primary production and bacterial production in offshore Antarctic waters during austral summer: coupled or uncoupled? Mar. Ecol. Prog. Ser. 222, 25–39.

Morán, X.A.G., Alonso-Sáez, L., 2011. Independence of bacteria on phytoplankton? Insufficient support for Fouilland & Mostajir's (2010) suggested new concept. FEMS Microbiol. Ecol. 78, 203–205. https://doi.org/10.1111/j.1574-6941.2011.01167.x.

Morán, X.A.G., Gasol, J.M., Pedrós-Alio, C., 2002. Dissolved primary production and the strength of phytoplankton bacterioplankton coupling in contrasting marine regions. Microb. Ecol. 44, 217–223.

Morán, X.A.G., Ducklow, H.W., Erickson, M., 2013. Carbon fluxes through estuarine bacteria reflect coupling with phytoplankton. Mar. Ecol. Prog. Ser. 489, 75–85. https://doi.org/10.3354/meps10428.

Piggott, J.J., Townsend, C.R., Matthaei, C.D., 2015. Reconceptualizing synergism and antagonism among multiple stressors. Ecol. Evol. 5, 1538–1547. https://doi.org/10.1002/ECE3.1465.

Regaudie-De-Gioux, A., Vaquer-Sunyer, R., Duarte, C.M., 2009. Patterns in planktonic metabolism in the Mediterranean Sea. Biogeosciences 6, 3081–3089.

Roshan, S., DeVries, T., 2017. Efficient dissolved organic carbon production and export in the oligotrophic ocean. Nat. Commun. 8, 2036. https://doi.org/10.1038/s41467-017-02227-3.

Sallée, J.B., Pellichero, V., Akhoudas, C., Pauthenet, E., Vignes, L., Schmidtko, S., Garabato, A.N., Sutherland, P., Kuusela, M., 2021. Summertime increases in upper-ocean stratification and mixed-layer depth. Nature 591, 592–598. https://doi.org/10.1038/s41586-021-03303-x.

Sandman, A.N., Wikström, S.A., Blomqvist, M., Kautsky, H., Isaeus, M., 2013. Scale-dependent influence of environmental variables on species distribution: a case study on five coastal benthic species in the Baltic Sea. Ecography 36, 354–363. https://doi.org/10.1111/J.1600-0587.2012.07053.X.

Santinelli, C., Ribotti, A., Sorgente, R., Gasparini, G.P., Nannicini, L., Vignudelli, S., Seritti, A., 2008. Coastal dynamics and dissolved organic carbon in the Western Sardinian shelf (western Mediterranean). J. Mar. Syst. 74, 167–188. https://doi.org/10.1016/j.jmarsys.2007.12.005.

Santinelli, C., Sempéré, R., van Wambeke, F., Charriere, B., Seritti, A., 2012. Organic carbon dynamics in the Mediterranean Sea: an integrated study. Glob. Biogeochem. Cy. 26, GB4004. https://doi.org/10.1029/2011GB004151.

Santinelli, C., Hansell, D.A., Ribera d'Alcalà, M., 2013. Influence of stratification on marine dissolved organic carbon (DOC) dynamics: the Mediterranean Sea case. Prog. Oceanogr. 119, 68–77. https://doi.org/10.1016/j.pocean.2013.06.001.

Santinelli, C., Iacono, R., Napolitano, E., Ribera d'Alcalá, M., 2021. Surface transport of DOC acts as a trophic link among Mediterranean sub-basins. Deep Sea Res. Pt I: Ocean. Res. Papers 170, 103493. https://doi.org/10.1016/j.dsr.2021.103493.

Sarmiento, J.L., Gruber, N., Brzezinski, M.A., Dunne, J.P., 2004. High-latitude controls of thermocline nutrients and low latitude biological productivity. Nature 427, 56–60. https://doi.org/10.1038/nature02127.

Serret, P., Robinson, C., Aranguren-Gassis, M., García-Martín, E.E., Gist, N., Kitidis, V., Lozano, J., Stephens, J., Harris, C., Thomas, R., 2015. Both respiration and photosynthesis determine the scaling of plankton metabolism in the oligotrophic ocean. Nat. Commun. 6, 1–10. https://doi.org/10.1038/ncomms7961.

Smith, D., Azam, F., 1992. A simple, economical method for measuring bacterial protein synthesis rates in seawater using 3H-leucine. Marine Microbial Food Webs 6, 107–114.

Statsoft, 2007. s.

Steemann-Nielsen, E., 1952. The use of radio-active carbon (C14) for measuring organic production in the sea. ICES J. Mar. Sci. 18, 117–140. https://doi.org/10.1093/icesjms/18.2.117.

Teira, E., Hernando-Morales, V., Fernández, A., Martínez-García, S., Álvarez-Salgado, X. A., Bode, A., Varela, M.M., 2015. Local differences in phytoplankton-bacterioplankton coupling in the coastal upwelling off Galicia (NW Spain). Mar. Ecol. Prog. Ser. 528, 53–69. https://doi.org/10.3354/meps11228.

Thingstad, T.F., Hagström, Å., Rassoulzadegan, F., 1997. Accumulation of degradable DOC in surface waters: is it caused by a malfunctioning microbial loop? Limnol. Oceanogr. 42, 398–404. https://doi.org/10.4319/lo.1997.42.2.0398.

van Wambeke, F., Lefèvre, D., Prieur, L., Sempéré, R., Bianchi, M., Oubelkheir, K., Bruyant, F., 2004. Distribution of microbial biomass, production, respiration, dissolved organic carbon and factors controlling bacterial production across a geostrophic front (Almeria-Oran, SW Mediterranean Sea). Mar. Ecol. Prog. Ser. 269, 1–15. https://doi.org/10.3354/MEPS269001.

van Wambeke, F., Taillandier, V., Deboeufs, K., Pulido-Villena, E., Dinasquet, J., Engel, A., Marañón, E., Ridame, C., Guieu, C., 2020. Influence of atmospheric deposition on biogeochemical cycles in an oligotrophic ocean system. Biogeosci. Discuss. 1–51 https://doi.org/10.5194/bg-2020-411.

Williamson, C.E., Neale, P., Hylander, S., Rose, K.C., Figueroa, F.L., Häder, D.-P., Wängberg, S.-Å., Worrest, R.C., 2019. The interactive effects of stratospheric ozone depletion, UV radiation, and climate change on aquatic ecosystems. Photochem. Photobiol. Sci. 18, 717–746.

Zhou, W., Li, Q.P., Wu, Z., 2021. Coastal phytoplankton responses to atmospheric deposition during summer. Limnol. Oceanogr. 66, 1298–1315. https://doi.org/10.1002/LNO.11683.